A COUPLED THERMO-ELECTRO-MECHANICAL MODEL FOR FRACTURE IN SOLAR CELLS

M. Paggi[a*], I. Berardone[b], M. Corrado[b]

[a]*IMT Institute for Advanced Studies Lucca, Piazza san Francesco 19, 55100 Lucca, Italy*
[b]*Politecnico di Torino, Department of Structural, Geotechnical and Building Engineering, corso Duca degli Abruzzi 24, 10129 Torino, Italy*
**marco.paggi@imtlucca.it*

Keywords: multi-physics; fracture mechanics; polycrystalline silicon; electroluminescence.

Abstract
Damage, micro-cracks, grain boundaries and other defects in solar cells are impacting on the electric power-loss and lifetime of photovoltaic modules, a complex example of a laminate structure. In the present contribution, a one-dimensional model for simulating the electric current distribution in solar cells accounting for a distributed series resistance is generalized to the presence of partially conductive cracks. The proposed model is used to perform a quantitative analysis of electroluminescence (EL) images of cracked monocrystalline silicon solar cells. A further generalization in a stochastic direction is also proposed in order to take into account randomly distributed defects typical of polycrystalline silicon. These developments represent a fundamental step towards the realization of an innovative fully coupled thermo-electro-mechanical numerical method for the study of fracture in solar cells and assessing the durability of photovoltaics.

1. Introduction

Cracking in Silicon solar cells is an important factor for the electrical power-loss of photovoltaic modules. Cracks on the millimeter or centimeter size, mostly invisible by naked eye, can lead to electrically inactive cell areas, thus reducing the power output of the module and the fill factor [1]. This takes place via the following mechanisms, i.e: a linear decreasing of the short circuit current by increasing the inactive cell area [2-4], and an increase in the series resistance of the cell due to cracking [2,5]. For instance, experimental results [5] have shown an increase in the series resistance of the cell of about 7% due to cracking with a corresponding power-loss of 4% and a fill factor reduction of 3%. Other experimental investigations [2] have shown that cracks inserted in solar cells by the application of a uniform pressure to simulate snow can lead up to 1.5% of power loss. After the subsequent application of 200 humidity freeze cycles according to standard specifications [6], such cracks propagate, the electrically disconnected areas increase in size and up to 10% of power loss has been reported. Potentially, if a crack crossing a conductor (called finger) is sufficiently open, then the finger may fail and the electric flow to the busbar in case of normal operating condition, or from the busbar in case of forward bias condition as in the EL testing, would be interrupted. Therefore, portions of Si cells can be potentially deactivated by cracks and their impact on power-loss reasonably depends on their inclination and position with respect to the

busbars, see Figs. 1(a) and (b). For instance, a crack parallel to the busbar on the upper side of the cell could lead up to 25% of electrically inactive area (Fig. 1(b)). According to this pure geometrical criterion which does not take into account neither physical mechanisms such as thermo-mechanical deformation, nor the fact that the cells are embedded in the composite PV module, worst-case scenarios have been predicted by considering all the experimentally detected [2] or numerically simulated [7] cracks as perfectly insulated lines. In reality, it is reasonable to expect intermediate configurations where cracks may partially conduct depending on the relative crack opening displacement at crack faces [8]. A complete modelling of the phenomenon should therefore consider the following steps: (i) simulation of crack nucleation and propagation according to a computational approach based on the cohesive zone model (CZM) [8]; (ii) analysis of thermal effects by augmenting the basic mechanical CZM to take into account the additional thermal resistance of cracks [9]; (iii) modelling of the electric response of the cell. A preliminary experimental observation supporting coupling effects induced by the thermo-mechanical field on the electric one due to cracking regards the highly oscillating electrical response in time of a PV string containing a cracked cell, depending on the cell temperature [10].

At present, electric models of solar cells do not consider this form of coupling induced by cracking. Usually, a discretization of the solar cell is made in the plane and a one-diode or a two-diodes models are applied to each node of the mesh to predict the electric response of the semiconductor [11,12]. In such approaches, the series resistance applied to each node is an equivalent one taking into account all different resistances (emitter, contact, metallization) However, it is independent on the position of the node with respect to the fingers and busbars grid. Recently, a one-dimensional model has been proposed taking into account the contribution of the grid conductivity to the distributed series resistance [13]. Nevertheless, so far, cracks and defects are never taken into account. In the present contribution, the one-dimensional model for current distribution is improved to consider the presence of cracks crossing the fingers grid. This is done by introducing a localized series resistance at the crack due to a partial opening of the crack faces. Also, the presence of randomly distributed defects is taken into account in a statistical sense, allowing a direct extension of the model to polycrystalline Si cells.

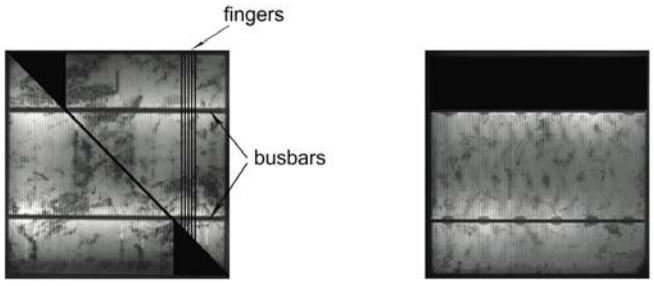

(a) 6% of potentially inactive cell (b) 25% of potentially inactive cell

Figure 1. Geometrical criterion showing the expected amount of potentially inactive cell areas depending on the orientation of the crack with respect to the busbars (a,b).

2. One-dimensional electric model with distributed series resistance

2.1. Electric model for undamaged monocrystalline Si cells

Recent studies have evidenced that the strongest spatial variation of the series resistance, R_s, in a Si cell is in the fingers grid direction, where the lateral series resistance is dominated by

the resistance of the grid lines [13]. On the contrary, the variation of R_s from grid line to grid line due to the emitter sheet resistance is smaller, and mainly due to a shadowing effect of the fingers. Therefore, the description of the distributed R_s of the whole cell may be analyzed with a one-dimensional model focusing on the variation of the grid line resistance. In this case, the electron current from busbar to busbar along a generic finger (see Fig. 2), is described by the following parameters: the vertical diode current density, I_v, with units of A/cm^2, the horizontal current density, I_h, with units of A/cm, and the voltage, V, having units of V. All these terms vary along the x coordinate (parallel to the finger's direction, as shown in Fig. 2). Without illumination, defining $I_h(x)$ as the horizontal current density at position x and $I_v(x)$ the vertical diode current density in the same position, as shown in Fig. 2, for each x the following equations hold:

$$\frac{\partial V(x)}{\partial x} = V'(x) = -\rho_s I_h(x) \tag{1}$$

$$\frac{\partial I_h(x)}{\partial x} = -I_v(x) \tag{2}$$

$$\frac{\partial^2 V(x)}{\partial x^2} = V''(x) = \rho_s I_v(x) \tag{3}$$

where $\rho_s = R_{grid} D$ is the sheet resistance in the x-direction, R_{grid} is the grid resistance (Ω/cm), and D is the distance between two grid lines. In the case of a low current density, I_v can be considered as constant. Therefore, Eq. (3) can be easily integrated over x and the well-known parabolic distribution is obtained for the voltage profile. On the other hand, if higher cell current values are considered, the local vertical current density is no longer a constant, and it should be computed from the following implicit equation:

$$I_v(x) = I_{01} \exp \frac{V(x) - R_{loc} I_v(x)}{n_1 V_T} - I_{sc} \tag{4}$$

where I_{sc} is the short circuit current density under illumination (I_{sc}=0 in the dark case), R_{loc} is the local sheet resistance, in series with the local diode (in undamaged monocrystalline Si cells it can be assumed as a homogeneous resistance within the whole cell, R_{hom}), I_{01} is the saturation current density, n_1=1 is the ideality factor, and V_T=kT/e is the thermal voltage.

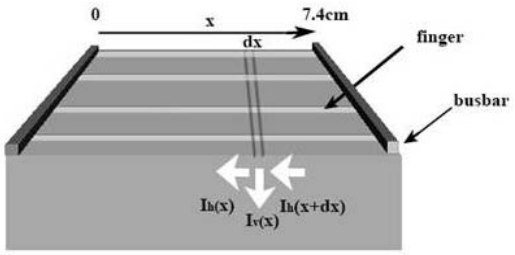

Figure 2. Schematic representation of investigated area with I_v and I_h vertical and horizontal current density, respectively.

Due to the implicit nature of Eq. (4), the voltage distribution along the grid line cannot be obtained in a closed form. On the other hand, Eq. (4) can be numerically solved using a Newton-Raphson method as proposed in [7], and Eqs. (1)-(3) can be numerically evaluated by

subdividing the integration path along the grid line into equidistant intervals of length dx. The vertical current density $I_v(x)$ is assumed constant within each interval. Under such an hypothesis, the voltage profile within the considered interval dx has still a parabolic shape, given by the following equations:

$$V(x+dx) = V(x) + V'(x)dx + \frac{V''(x)}{2}dx^2 \tag{5}$$

$$V'(x+dx) = V'(x) + V''(x)dx \tag{6}$$

In the case of undamaged monocrystalline Si cells, due to symmetry reasons, the starting point for the step-by-step integration process is the middle position between the two busbars (x_0=3.7 cm with reference to the scheme in Fig. 2). Hence, the starting boundary conditions in this point are given by symmetry conditions:

$$V(x_0) = V_0;\ V'(x_0) = 0;\ I_h(x_0) = 0 \tag{7}$$

Starting from x=x_0 and going towards one of the two busbars (a symmetric behavior is expected), the value of the vertical current density I_v is computed from Eq. (4). Then, the values of the local voltage V(x+dx) and its gradient V'(x+dx) at the end of each interval are computed from Eqs. (5) and (6), by substitution of Eqs. (1) and (3). Analogously, the increment of I_h within each interval is given by the following equation:

$$I_h(x+dx) = I_h(x) + I_v(x)dx \tag{8}$$

Note that the direction of integration is opposite to the direction of electron current (arrows in Fig. 2) and we consider dark conditions. Therefore, both V' and V'' are positive. Applications of this approach to intact monocrystalline cells (no-discontinuities in the current flow along the grid line) have been proposed in [12].

2.2. Generalization of the electric model in case of cracks

The presence of a crack crossing a Si cell and the fingers grid determines a discontinuity in mechanical, thermal, and electric fields. In the latter case, in fact, the crack introduces an additional resistance along the current path that influences the distribution of the vertical and the horizontal current densities, as well as that the voltage distribution. The value of such a resistance, in the following referred to as R_{cr}, is presumably related to the value of the crack opening displacement: the largest is the crack opening the highest is the electric resistance. The effects of a crack on the distribution of the vertical diode current density, I_v, within a cell is evident from the analysis of the EL image of a cracked cell. The brightness of the EL image, in fact, is proportional to I_v [14]. When the crack opening displacement is sufficiently large, a discontinuity in the grey-scale is evidenced on the opposite sides of the crack.

The one-dimensional electric model proposed in [13] and outlined in the previous section, is herein extended to consider the presence of a crack. To this aim, a discontinuity in the voltage distribution along the grid line is introduced in correspondence of the crack, x_{cr}:

$$V(x_{cr}^+) = V(x_{cr}^-) + R_{cr} I_h(x_{cr}) \tag{9}$$

Then, the same step-by-step procedure previously outlined is applied, with some modifications in the application of the boundary conditions. In this case, in fact, symmetry conditions are no longer valid, and different considerations have to be done in order to select the starting point x0, of the integration path. In this approach, it is selected in order to obtain, as a result of the integration process, the same value of the voltage in correspondence of the two busbars. The boundary conditions defined in Eq. (7) are applied in the position x0 and the step-by-step integration procedure is applied twice, once towards the left-hand busbar and once towards the right-hand busbar. The jump in the voltage given by Eq. (9) is applied when, along the integration path, the crack is intercepted. The same approach can be pursued in case two cracks are crossing the fingers' grid. The starting point will be in the portion between the two cracks and, therefore, a jump in the voltage will be considered along both the integration paths.

The proposed method is applied to pre-cracked monocrystalline Si cells embedded in semi-flexible modules made of 2 rows of 5 cells (see [15] for more details). Loaded and unloaded conditions have been considered in order to change the stress field in the cells. The application of a bending stress to the panel, in fact, determined an increase of the crack opening displacement of the pre-existing cracks. The distribution of the vertical diode current density, I_v, and the voltage along a selected grid line, obtained by the numerical model, is reported in Fig. 3 for a finger crossed by one crack. The parameters assumed for all the simulations are: I_{sc}=0, R_{loc}=0.2 Ωcm^2, V_T=25 mV, ρ_s=0.138 Ω, I_{01}=1.48x10^{-12} mA/cm^2. The value of the other parameters, specific for each simulation, are reported in the captions of Fig. 3. The vertical current density is compared to the distribution of the EL along the same grid line, suitably rescaled by a scale factor (black dots in Figs. 3a and 3b, for unloaded and loaded condition, respectively). The numerically simulated I_v fits very well the experimental current determined from the EL data. The localized resistance due to the crack is just considered here as a free parameter as x_0 and V_0, used to better fit the EL experimental data and to obtain the same voltage in correspondence of the two busbars at x=0 and x=7.4 cm. Future developments will regard the correlation between this localized resistance and the crack opening. The same analysis has been done along a finger belonging to the same Si cell but crossed by two cracks, see Fig. 4. Again, an excellent matching with experimental data is shown.

3. Electric model with spatially inhomogeneous series resistance

In polycrystalline Si cells, the local resistance, R_{loc}, is dishomogeneous and depends on grain boundaries and defects. This is clearly evidenced by a close analysis of a EL image, such that shown in Fig. 5a. The distribution of the brightness within the image does not depend only on the distance from the busbars as for monocrystalline Si (Fig. 5b), but several darker spots, representing grain boundaries and defects, are randomly distributed within the cell. In this case, the proposed model can be applied by introducing a spatially inhomogeneous series resistance instead of the homogeneous R_{loc}. Such a resistance can be defined as R_{ave}+dR, where R_{ave} is the average value and dR takes into account the fluctuations/perturbations using pseudo-random values taken from a Gaussian distribution with a prescribed variance.

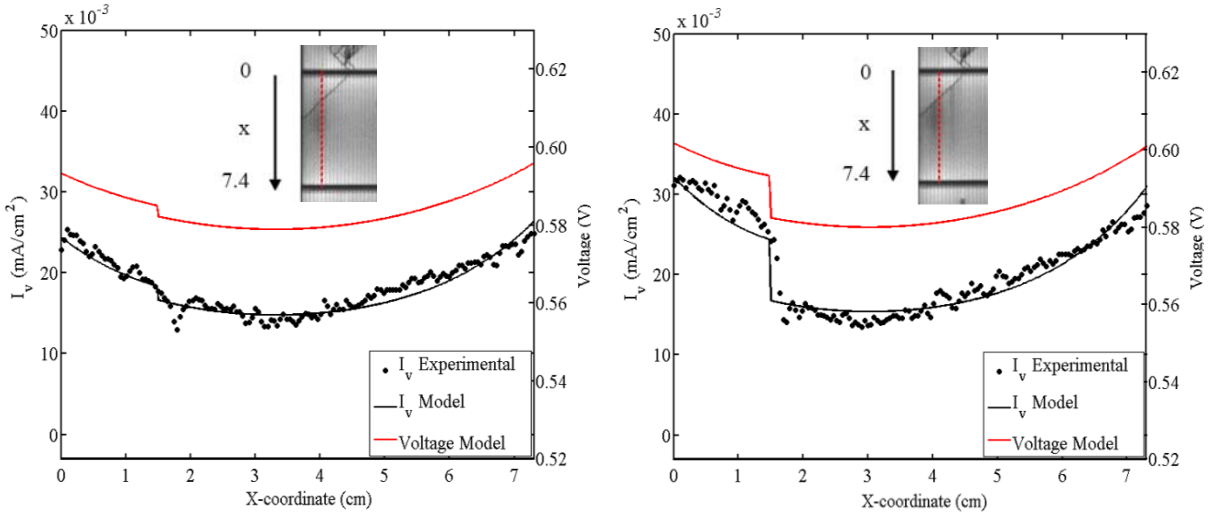

(a) Unloaded condition. (x_0=3.33 cm, V_0=0.579 V, R_{cr}=0.096 Ωcm^2)

(b) Loaded condition. (x_0=3.03 cm, V_0=0.580 V, R_{cr}=0.22 Ωcm^2)

Figure 3. Vertical current and voltage in a monocrystalline Si cell along a finger crossed by one crack: (a) unloaded and (b) loaded conditions.

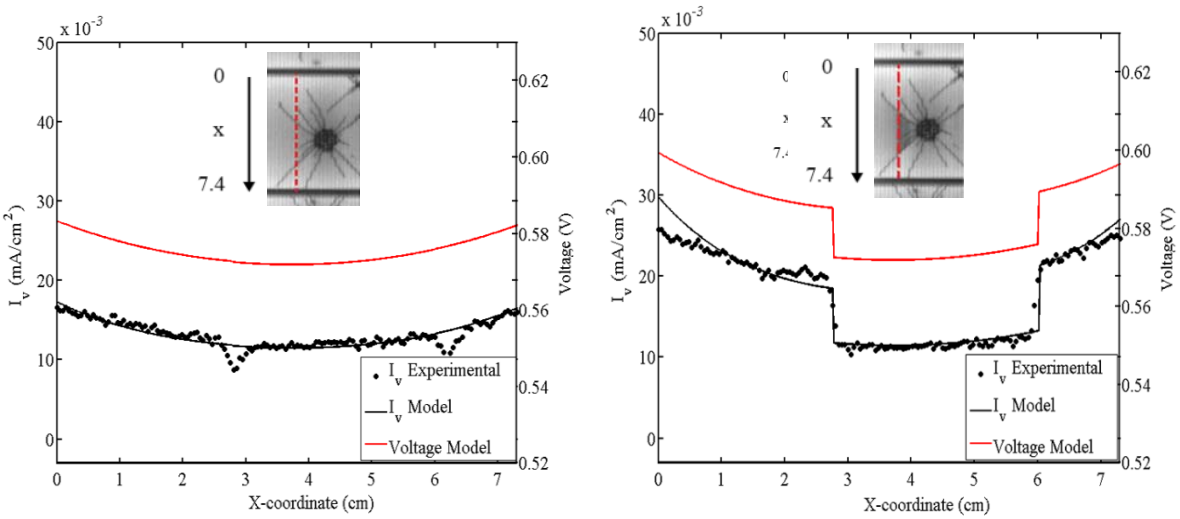

(a) Unloaded condition. (x_0=3.73 cm, V_0=0.572 V, R_{cr1}=R_{cr2}=0.0 Ωcm^2)

(b) Loaded condition. (x_0=3.72 cm, V_0=0.572 V, R_{cr1}=1.13 Ωcm^2, R_{cr2}=0.48 Ωcm^2)

Figure 4. Vertical current and voltage in a monocrystalline Si cell, along a finger crossed by two cracks: (a) unloaded and (b) loaded conditions.

The model has been applied along a grid line of an intact and a cracked polycrystalline cell, and the obtained vertical current densities are shown in Figs. 6a and 6b, respectively, compared to the experimental data. In particular, both the I_v distributions obtained by considering only R_{ave} and R_{ave}+dR are shown. A good matching with experimental data is obtained by assuming an amplitude of the perturbative term, dR, of about 30% the average value, R_{ave}.

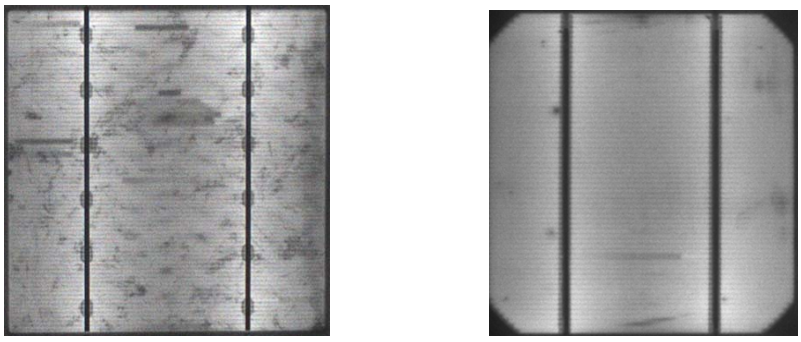

(a) Polycrystalline Si cell (b) Monocrystalline Si cell

Figure 5. Electroluminescence images of intact mono- and polycrystalline Si cells.

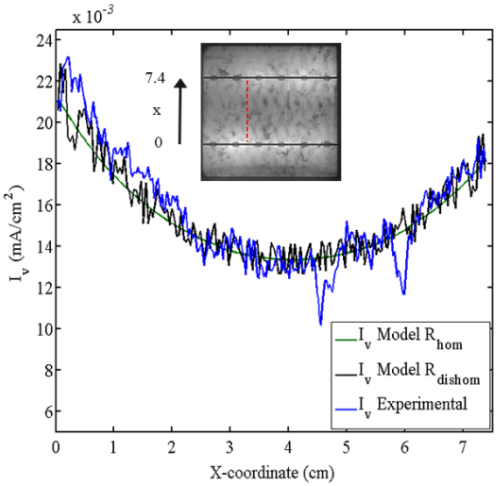

(a) Intact polycrystalline Si cell. (x_0=4.07 cm, V_0=0.58 V, R_{ave}=0.5 Ωcm^2, dR=30%)

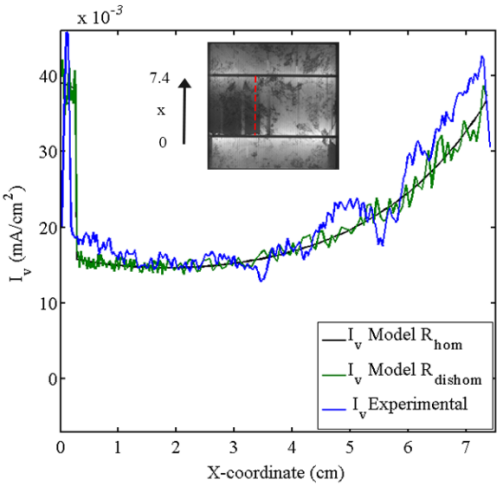

(b) Cracked polycrystalline Si cell. (x_0=1.85 cm, V_0=0.58 V, R_{ave}=0.5 Ωcm^2, dR=30%, R_{cr}=1.4 Ωcm^2)

Figure 6. Vertical current along a finger in a (a) intact and (b) cracked polycrystalline Si cell.

4. Conclusions

In the present study, the one-dimensional model for current distribution in [13] has been generalized to the presence of cracks. The proposed method can be used to interpret the relation between voltage discontinuity and crack opening displacement at crack faces, correlating the crack opening, predicted according to nonlinear computational fracture mechanics simulations, and the localized resistance induced by the crack. In monocrystalline Si cells, the influence of crack opening on the electric response is evident, since the value of R_{cr} significantly increases by bending the module (see Figs. 3,4). In case of polycrystalline silicon, the scenario is much more complex due to a voltage fluctuation caused by the contemporary presence of defects, grain boundaries and imperfections. Therefore, the use of a stochastic approach to model the local series resistance should be taken into account, as herein proposed.

Acknowledgements

The research leading to these results has received funding from the European Research Council under the European Union's Seventh Framework Programme (FP/2007–2013)/ERC Grant Agreement No. 306622 (ERC Starting Grant "Multi-field and multi-scale

Computational Approach to Design and Durability of PhotoVoltaic Modules" – CA2PVM). The support of the Italian Ministry of Education, University and Research to the Project FIRB 2010 Future in Research "Structural mechanics models for renewable energy applications" (RBFR107AKG)

References

[1] M.A. Green. *Solar Cells*, Prentice-Hall Inc. Englewood Cliffs, N.J., USA, 1982, pp. 97.
[2] M. Köntges, I. Kunze, S. Kajari-Schröder, X. Breitenmoser and B. Bjrneklett. The risk of power loss in crystalline silicon based photovoltaic modules due to microcracks. *Solar Energy Materials and Solar Cells*, 95:1131-1137, 2011.
[3] K.-H. Kim, S. Kasouit, E.V. Johnson and P. Roca i Cabarrocas. Substrate versus superstrate configuration for stable thin film silicon solar cells. *Solar Energy Materials and Solar Cells* 119:124-128, 2013.
[4] K.-H. Kim, E.V. Johnson, P. Roca i Cabarrocas. Irreversible light-induced degradation and stabilization of hydrogenated polymorphous silicon solar cells. *Solar Energy Materials and Solar Cells* 105:208-212, 2012.
[5] R. Khatri, S. Agarwal, I. Saha, S.K. Singh and B. Kumar. Study on long term reliability of photo-voltaic modules and analysis of power degradation using accelerated aging tests and electroluminescence technique. *Energy Procedia*, 8:396-401, 2011.
[6] International Standard IEC 61215:2006. Crystalline Silicon Terrestrial Photovoltaic (PV) Modules – Design Qualification and Type Approval, 2006.
[7] M. Paggi, M. Corrado and M.A. Rodriguez. A multi-physics and multi-scale numerical approach to microcracking and power-loss in photovoltaic modules. *Composite Structure*, 95:630-638, 2013.
[8] A. Infuso, M. Corrado, M. Paggi. Image analysis of polycrystalline solar cells and modelling of intergranular and transgranular cracking. *Journal of the European Ceramic Society*, doi:10.1016/j.jeurceramsoc.2013.12.051
[9] M. Paggi and A. Sapora. Numerical modelling of microcracking in PV modules induced by thermo-mechanical loads. *Energy Procedia* 38:506-515, 2013.
[10] B. Weinreich, B. Schauer, M. Zehner and G. Becker. Validierung der Vermessung gebrochener Zellen im Feld mittels Leistungs PV-Thermographie. In *Proc. 27 Symposium Photovoltaische Solarenergie*, 190-196, 2012.
[11] D. Grote. *Analyses of silicon solar cells and their measurement methods by distributed, circuit simulations and by experiment*. PhD thesis, University of Konstanz, Germany, 2010.
[12] S. Guo, F.-J. Ma, B. Hoex, A.G. Aberle and M. Peters. Analysing Solar Cells by Circuit Modelling, *Energy Procedia* 25:28-33, 2012.
[13] O. Breitenstein and S. Rißland. A two diode model regarding the distributed series resistance. *Solar Energy Materials and Solar Cell*, 110:77-86, 2013.
[14] T. Fuyuki, H. Kondo, Y. Kaji, A. Ogane and Y. Takahashi. Analytic findings in the electroluminescence characterization of crystalline silicon solar cells. *Journal of Applied Physics*, 101:023711, 2007.
[15] M. Paggi, I. Berardone, A. Infuso, M. Corrado. Fatigue degradation and electric recovery in Silicon solar cells embedded in photovoltaic modules. *Scientific Reports* 4, 4506; DOI:10.1038/srep04506, 2014.